

1 Confirmation and fine mapping of the resistance 2 locus *Ren9* from the grapevine cultivar ‘Regent’

3 Daniel Zendler¹, Reinhard Töpfer¹, Eva Zyprian^{1*}

4 ¹ Julius Kühn-Institute, Institute for Grapevine Breeding Geilweilerhof, Siebeldingen, Germany

5 * Correspondence: eva.zyprian@julius-kuehn.de; Tel.: +49 6345 41126 orcid.org/0000-0003-1095-1996

6 **Abstract:** Grapevine (*Vitis vinifera* ssp. *vinifera*) is a major fruit crop with high
7 economic importance. Due to its susceptibility towards fungal pathogens such as
8 *Erysiphe necator* and *Plasmopara viticola*, the causal agents of powdery and downy
9 mildew (PM, DM), grapevine growers annually face a major challenge in coping
10 with shortfall of yield caused by these diseases. Here we report the confirmation of
11 a genetic resource for grapevine resistance breeding against PM. During the
12 delimitation process of *Ren3* on chromosome 15 from the cultivar ‘Regent’, a
13 second resistance-encoding region on chromosome 15 termed *Ren9* was
14 characterized. It mediates a trailing necrosis associated with the appressoria of *E.*
15 *necator* and restricts pathogen growth. In this study, we confirm this QTL in a related
16 mapping population of ‘Regent’ x ‘Cabernet Sauvignon’. The data show that this
17 locus is located at the upper arm of chromosome 15 between markers GF15-58
18 (0.15 Mb) and GF15-53 (4 Mb). The efficiency of the resistance against one of the
19 prominent European PM isolates (EU-B) is demonstrated. Based on fine-mapping
20 and literature knowledge we propose two possible regions of interest and supply
21 genetic markers to follow both regions in marker assisted selection.

22 **Keywords:** Breeding, *E. necator*, grapevine, necrosis, powdery mildew, R-genes,
23 *Ren9*, resistance, *V. vinifera*

24 1. Introduction

25 The era of accelerated plant breeding started with the emergence of marker-
26 assisted selection (MAS). With this tool in hand, breeders dealing with woody
27 perennials became able to select promising progeny with the desired characteristics
28 at the very early seedling (cotyledon) stage. In grapevine, the requested
29 characteristics are primarily resistance traits against several pathogens, as
30 viticulture worldwide is threatened by a variety of different pests [1,2]. One of the
31 most prominent diseases in vineyards is powdery mildew (PM) caused by the
32 obligate biotrophic ascomycete *Erysiphe necator* (syn. *Uncinula necator* (Schw.)

33 Burr; anamorph *Oidium tuckeri* Berk). This pathogen occurs predominantly in dry
34 and warm regions. *E. necator* is able to grow on the surface of all green tissues of
35 the cultivated grapevine *Vitis vinifera* ssp. *vinifera* (*V. vinifera*). The highest damage
36 is caused by infection of unripe berries. At this stage, PM infestation provokes the
37 growing berries to crack open providing entry points for any secondary bacterial and
38 / or fungal infections eventually leading to rotting of the bunches [3,4].

39 Roughly 170 years ago, *E. necator* was one of the three grapevine-pests
40 introduced to Europe by trading of grapevines derived from crosses of native North
41 American *Vitis* species with *V. vinifera* by England, France and Spain and America
42 [1]. This was the first encounter of *V. vinifera* with this already highly adapted
43 grapevine pathogen on the Eurasian continent explaining the high susceptibility of
44 the cultivated grapevine towards PM. The combination of the pathogenic insect
45 phylloxera (*Daktulosphaira vitifoliae*), an obligate biotrophic oomycete causing
46 downy mildew (*Plasmopara viticola*; DM) and PM was responsible for the collapse
47 of wine production in France and Spain roughly 150 years ago [1]. The soil borne
48 stage of phylloxera infests the roots of grapevines causing damage and entry points
49 for secondary infections. This results in low yield and eventually in dieback of
50 infested grapevines after several seasons [5]. In addition, the two mildews infect all
51 green tissues of the grapevine. Infections early in the season can lead to complete
52 loss of harvest if DM and PM infect young flowers. The phylloxera-problem was
53 solved by the invention of “crafting” the high wine-quality scions on phylloxera-
54 resistant *Vitis* hybrid rootstocks. Protection against the two mildews was achieved
55 by the invention of the “Bordeaux mixture”, a mixture of Sulphur- and Copper-
56 compounds that prohibits the development of DM and PM when applied prior to
57 infections [6]. This mixture was so effective that even today, 170 years later, it still
58 plays a central role in the plant protection regime of most viticulturists, including
59 organic wine growers. However, to achieve effective plant protection for the highly
60 PM and DM susceptible *V. vinifera* cultivars, fungicides such as the Sulphur- and
61 Copper-compounds or other synthetic protectants have to be applied depending on
62 the environmental conditions up to 12 times during the growing season [7]. This
63 makes viticulture one of the highest agricultural consumers of fungicides [8].
64 Furthermore, these applications make viticulture laborious and are harmful for
65 humans and the environment due to residues on grape clusters and rain wash-off
66 from plants after treatment [9,10]. On top, an unambiguous correlation of wine

67 growing regions and copper accumulation in top soils was shown. This Copper can
68 be washed off into the nearby rivers and damage non-target organisms [11].

69 One way to reduce the enormous amounts of fungicides used in viticulture is to
70 breed novel resistant grapevine cultivars carrying resistance traits against DM and
71 PM combined with high wine quality [1,12]. Due to co-evolution of DM and PM with
72 wild *Vitis* species in North America, some accessions of these species have evolved
73 natural genetic resistances which either inhibit the growth of the pathogen partially
74 or completely. In the last decades, roughly 13 of such natural genetic resistance loci
75 against PM have been identified [13–15]. They were delimited to certain regions on
76 various chromosomes of the grapevine genome. Such loci are exploitable by
77 grapevine breeders for introgression into new cultivars with the assistance of MAS.
78 However, it is crucial for breeders to know which resistances to stack to achieve the
79 most durable effect against PM. Therefore, a detailed characterization of the
80 individual resistance loci and their function is essential. This requires artificial
81 inoculation experiments followed by evaluation at different time points of
82 pathogenesis [16].

83 The resistance locus *Ren9* was identified during a fine-mapping study of the
84 resistance locus *Ren3* on chromosome 15 of ‘Regent’ [15]. It is located in the anterior
85 part of chromosome 15 spanning an interval of roughly 2.4 Mb. To confirm this locus
86 and possibly further delimit the resistance-mediating region on chromosome 15, a
87 cross of ‘Regent’ and ‘Cabernet Sauvignon’ was phenotypically characterized
88 repeatedly throughout the growing season of 2016. In addition, controlled
89 experimental inoculations were performed with selected F₁ genotypes from that
90 cross that carry meiotic recombinations within chromosome 15. In the frame of this
91 work new genetic insertion / deletion (Indel) markers were designed spanning the
92 previously delimited region for *Ren9* with a spacing of 0.1 – 0.2 Mb. These markers
93 allow a possible further delimitation of the resistance locus *Ren9* on chromosome 15
94 in the grapevine genome.

95

96

97

98

99

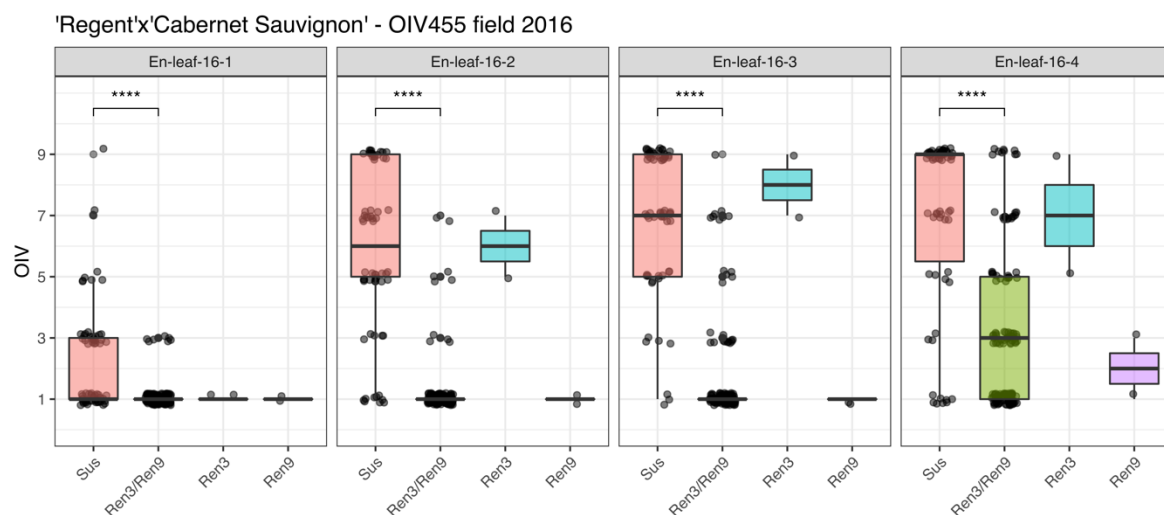
100

101 2. Results

102 2.1 Phenotypic field-data

103 Phenotypic data from the cross population of 'Regent' x 'Cabernet Sauvignon'
104 were recorded four times during the growing season 2016. This approach was
105 chosen since previous phenotypic evaluations that had been performed at the end
106 of each season yielded scores of around 5 to 9 for nearly all genotypes (whether
107 they were resistant or susceptible) and were blurring genetic differences due to the
108 late evaluation date. The same approach was applied earlier in the cross population
109 of 'Regent' x 'Lemberger', which allowed the observation of shifting QTLs during the
110 season [15]. According to their genotypic profiles the F1 individuals were grouped in
111 either resistant (*Ren3-Ren9*) or susceptible and individuals with either *Ren3* ("*Ren3*-
112 only") or *Ren9* ("*Ren9*-only"). The distribution of phenotypic data is visualized in
113 Figure 1. The significance of the difference between resistant und susceptible
114 genotypes is indicated above the boxplots (Figure 1). Differences between *Ren3* and
115 *Ren9* carrying F1 individuals were not further investigated due to the fact that these
116 two groups are represented by only two individuals each (Figure 1).

117



119

120 Figure 1: Boxplots of assigned phenotypic scores for the genotypic groups of 'Regent' x 'Cabernet
121 Sauvignon'. Boxes indicate the interquartile range. The median for the respective dataset is indicated
122 by a horizontal line in the boxplot. Number of individuals: susceptible (sus) n=62, Ren3/Ren9 n=132,
Ren9 n=2, Ren3 n=2. (***) = $P \leq 0.001$, (**) = $P \leq 0.01$, (*) = $P \leq 0.05$, NS = not significant $P > 0.05$)

123

124 The phenotypic scores in the first scoring date are shifted towards 1 as the
125 medians indicate in the boxplots (Figure 1). The main distribution of phenotypic

126 scores ranged from 1 to 5 in this dataset which was due to the early date of scoring.
 127 However, significant differences could be detected between susceptible and
 128 resistant genotypes (Figure 1, 16-1: sus – Ren3-Ren9 ***). The median of
 129 susceptible genotypes is continuously shifted towards 9 in the three following
 130 datasets (Figure 1, 16-2, 16-3, 16-4). For genotypes with *Ren3* and *Ren9* associated
 131 alleles the median shifts to 3 in the last dataset which represents the scoring date at
 132 the end of the season with highest infection pressure (Figure 1, 16-4). The two
 133 individuals with only *Ren3* also show a continuous shift towards score 7, indicating
 134 a rather strong infestation with *E. necator* (Figure 1, 16-4). In contrast, for the two
 135 individuals carrying *Ren9*, the median score is shifted to score 2 at the last date
 136 (Figure 1, 16-4).

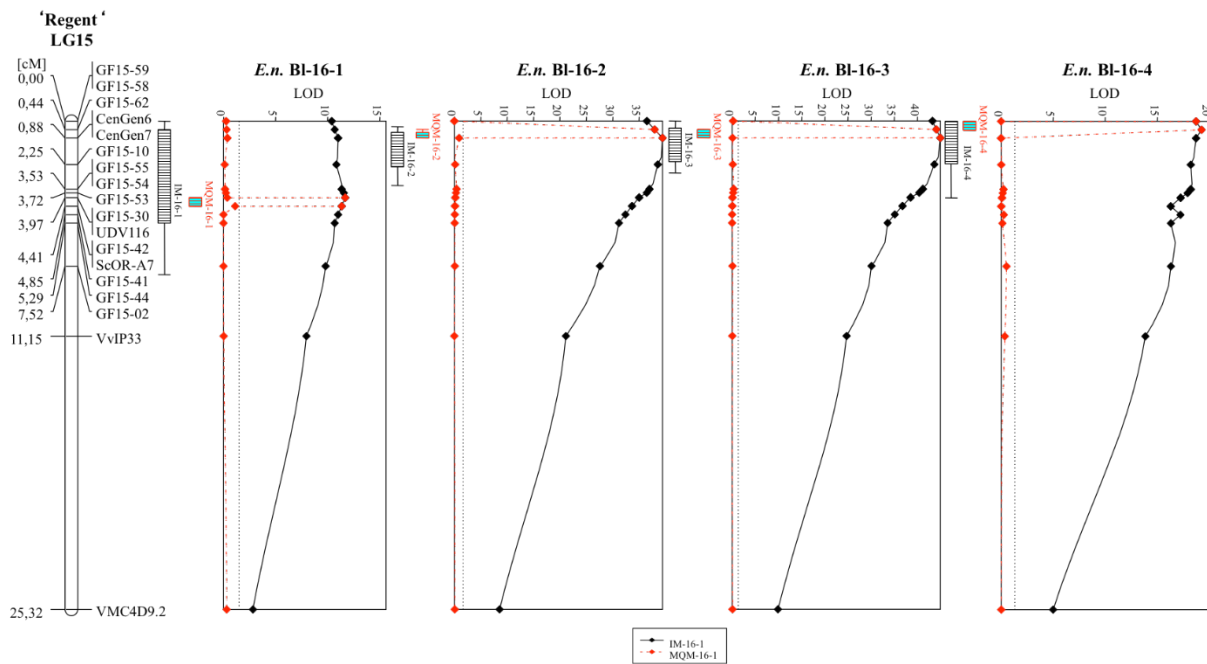
137 2.2 QTL-analysis with phenotypic field-data

138 The described phenotypic data was used for QTL-analysis with the previously
 139 published genetic map of ‘Regent’ x ‘Cabernet Sauvignon’ [15]. QTL analysis was
 140 performed with the maternal (‘Regent’) and paternal (‘Cabernet Sauvignon’) genetic
 141 map. Therefore, the genotypic data was coded as doubled haploid (DH) according
 142 to the manual of JoinMap®4.1. Results for the ‘Regent’ haplophase are listed in
 143 Table 1 and are shown as graph in Figure 2. The results for the ‘Cabernet Sauvignon’
 144 haplophase are shown in Figure S1. In this haplophase no LOD score higher than 3
 145 was detected and therefore this haplophase was not further investigated. For all
 146 scoring dates, a QTL for resistance to powdery mildew was observable on
 147 chromosome 15 (Table 1, Figure 2).

148

149 Table 1: QTL-analysis results for PM resistance scored at four different times of the epidemic (E.n.—
 150 leaf-16-1 to 16-4) together with the genetic map of LG15 of ‘Regent’.

	Data	Mapping	LOD _{max}	% Expl	Nearest Marker	QTL-interval (LOD _{max} ±1)	LG15 LOD p≤0,05	Interval [Mb]
‘Regent’ LG15	<i>E.n.-leaf-16-1</i>	IM	11,96	23,1	GF15-30/UDV116	GF15-62 - GF15-44	1,3	8,7
		MQM	11,96	23,1	UDV116	UDV116 - ScORA7		3.1
	<i>E.n.-leaf-16-2</i>	IM	39,47	58,6	CenGen6/CenGen7	CenGen6 - GF15-10	1,2	0.8
		MQM	39,47	58,6	CenGen6	GF15-62 - CenGen7/6		0.2/0.5
	<i>E.n.-leaf-16-3</i>	IM	44,96	63,8	CenGen6/CenGen7	GF15-62 - CenGen7/6	1,3	0.2/0.5
		MQM	44,96	63,8	CenGen6	GF15-62 - CenGen7/6		0.2/0.5
	<i>E.n.-leaf-16-4</i>	IM	19,25	34,7	GF15-62	GF15-59/58 - GF15-54/55	1,2	2.7
		MQM	19,25	34,7	GF15-62	GF15-59/58 - GF15-62		0.9



151

152 Figure 2: QTL graphs for the four analyzed scoring dates in 2016 with the genetic map of 'Regent'
153 derived from the 'Regent' x 'Cabernet Sauvignon' mapping population. The continuous black line
154 shows the results of IM while the dotted red line indicates the MQM results. The confidence intervals
155 of +/-1 and +/-2 LOD values are indicated by the box and its whiskers at the left side of each graph.

156

157 The first scoring (*E.n.*-leaf-16-1) yielded a rather low LOD value of approximately
158 12 compared to the later three scoring dates (Table 1, Figure 2). This QTL explained
159 around 23% of the observed phenotypic variation. The interval mapping (IM) analysis
160 pointed to an interval spanning the region between markers GF15-62 and GF15-44
161 (Table 1). This represents around 8.7 Mb of chromosome 15 according to the
162 reference genome PN40024 12X v2. The following MQM mapping limited the region
163 to the interval around UDV116 to ScORA7 (3.1 Mb) with UDV116 being the nearest
164 correlating marker (Table 1, Figure 2). The subsequent scoring dates yield QTLs
165 with LOD_{max} scores of 39 (*E.n.*-leaf-16-2) and 45 (*E.n.*-leaf-16-3) and explained up
166 to 63% of observed phenotypic variation (Table 1). The intervals of the IM analysis
167 were limited to CenGen6 – GF15-10 for *E.n.*-leaf-16-2 (0.8 Mb) and to GF15-62 –
168 CenGen7/6 for *E.n.*-leaf-16-3 (0.2/0.5 Mb). Downstream MQM analysis limited the
169 interval for both scoring dates to the region between GF15-62 and CenGen7/6
170 representing 0.2 resp. 0.5 Mb on chromosome 15 (Table 1, Figure 2). The forth
171 scoring yielded a QTL, which was shifted completely to the beginning of
172 chromosome 15 (Figure 2). This QTL was represented by a LOD_{max} score of 19 and
173 represented 35% of observed phenotypic variance (Table 1). The interval of this QTL

174 spanned the genetic markers GF15-59/58 and GF15-54/55 that corresponds to 2.7
 175 Mb. Subsequent MQM mapping limited the interval to GF15-59/58 – GF15-62 (Table
 176 1). Taken together, a shift of the QTL from the middle part (*Ren3*) to the anterior part
 177 (*Ren9*) of chromosome 15 is observed during the time of beginning of the season to
 178 its end.

179 2.3 Fine mapping of the *Ren9* region in leaf disc assays

180 Controlled infection assays were done with leaf discs from selected F1
 181 individuals (Table 2) chosen according to their meiotic recombination points on
 182 chromosome 15.

183 Table 2: Individuals from the cross 'Regent' x 'Cabernet Sauvignon' with meiotic recombinations on
 184 chromosome 15. SSR-Markers and newly designed Indel-markers are shown: resistance associated
 185 allele (+), no resistance associated allele (-), marker not called (?). Together with the recombination
 186 points the inverse OIV455 scorings (1 - highly resistant, 9 – highly susceptible) are shown. Genetic
 187 markers in regions of *Ren3* ([15], GF15-42, ScOR-A7, GF15-41) and *Ren9* (Indel-27, Indel-23, Indel-
 188 17) are marked in grey.

Loci		<i>Ren9</i>	<i>Ren9</i>	<i>Ren9</i>	<i>Ren3/ Ren9</i>	<i>Ren3/ Ren9</i>	<i>Ren3/ Ren9</i>	<i>Ren3/ ?Ren9?</i>	<i>Ren3</i>	<i>Ren3</i>
PN [Mb]	Marker	1999- 074-068	1999- 074-117	1999- 074-129	1999- 074-062	1999- 038-017	1999- 074-122	1999- 074-239	1999- 074-204	1999- 074-136
1.1	CenGen7	+	+	+	+	+	+	-	-	-
1.2	Indel-19	+	+	+	+	+	+	-	-	-
1.7	Indel-20	+	+	+	+	+	+	-	-	-
2.0	Indel-24	+	+	+	+	+	+	-	-	-
2.1	Indel-29	+	+	+	+	+	+	-	-	-
2.2	Indel-27	+	+	+	+	+	+	+	-	-
2.4	Indel-23	+	+	+	+	+	+	+	-	-
2.6	Indel-17	+	+	+	+	+	+	+	-	-
2.9	Indel-13	+	+	+	+	+	+	+	+	+
3.5	GF15-53	-	?	+	+	+	+	+	+	+
3.8	GF15-54	-	+	+	+	?	?	+	?	+
4	GF15-55	-	?	+	+	+	+	+	?	+
6.3	UDV116	-	+	+	+	+	?	+	+	+
7	GF15-30	-	?	+	+	+	?	+	+	+
9.3	GF15-42	-	-	-	+	+	+	+	+	+
9.3	ScOR A7	-	-	-	+	+	+	+	+	+
9.6	GF15-41	-	-	-	-	+	+	+	+	+
9.9	GF15-44	-	-	-	-	+	+	+	+	+
11.6	GF15-02	-	-	-	-	+	+	+	+	+
13	VvIP33	-	-	-	-	+	+	+	+	+
16.6	VMC4D9.2	-	-	-	-	+	+	+	+	+
OIV 455	16-1	1	1	1	1	1	1	1	1	1
	16-2	1	1	1	1	1	1	1	7	5
	16-3	1	NA	1	1	1	3	1	9	7
	16-4	3	NA	1	9	3	1	1	9	5
	Average	1.5 SE±0.5	1 SE±0	1 SE±0	3 SE±2	1.5 SE±0.5	1.5 SE±0.5	1	6.5 SE±1.9	4.5 SE±1.3
Avr. / locus	1.1667, SE ± 0.167			2, SE ± 0.34			1	5.5, SE ± 1		

189

190 For delimiting the region around *Ren9*, new genetic markers were designed
 191 based on insertions and deletions. Table 2 presents the recombination points of the

192 selected F1 genotypes from the ‘Regent’ x ‘Cabernet Sauvignon’ cross.
 193 Oligonucleotide sequences and amplicons are shown in Sup. Table 1. Individuals
 194 with *Ren3/Ren9* and “*Ren9*-only” show an average OIV 455 score of 1.7 and 1.16,
 195 respectively (Table 2). Assuming the location of the resistance conferring gene of
 196 *Ren9* in the interval from CenGen7 to Indel-13, two of the recombinants show only
 197 *Ren3* associated alleles. These exhibit an average OIV 455 score of 5.5 (Table 2).
 198 In contrast to the two “*Ren3* only” individuals, the F1 plant 1999-074-239 shows
 199 resistance associated alleles for the markers Indel-27, Indel-23 and Indel-17 and an
 200 average phenotypic score of 1.0 (Table 2).

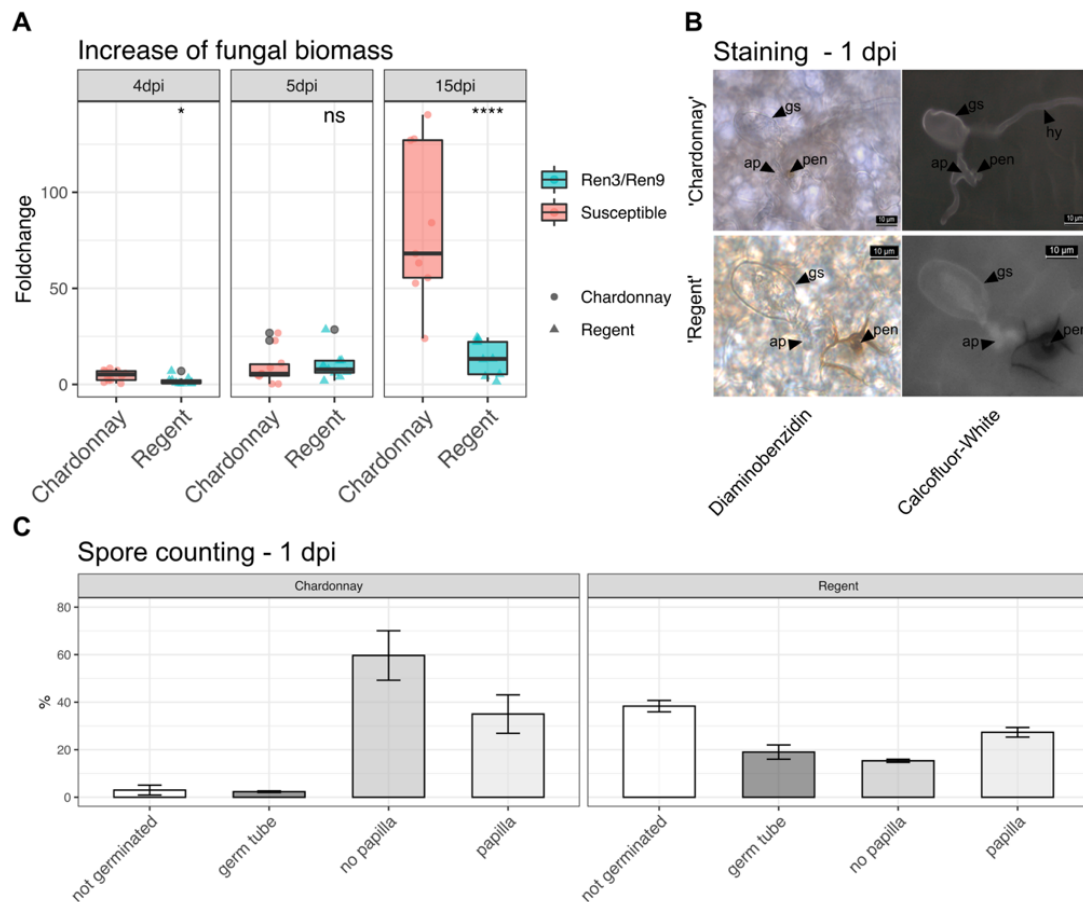
201 2.4 Characterizing the PM single spore isolate GF.En-01

202 For controlled infection phenotyping, leaf disc inoculation experiments were
 203 performed with the aforementioned F₁ individuals and a single spore PM isolate,
 204 GF.En-01. The latter was sampled from a susceptible grapevine cultivar around the
 205 JKI Institute for Grapevine Breeding Geilweilerhof, Germany. Genotyping of this
 206 isolate showed that it is most likely of EU-B type according to the identified and
 207 translated allele sizes described [17] (Table 3). There was some uncertainty for the
 208 allele sizes of EnMS-03 and -06 as they differed more than 2 bp from the published
 209 sizes (Table 3).

210 Table 3: Allele sizes of the PM isolate GF.En-01 for EnMS markers [27]. Genetic markers with
 211 uncertain allele results are marked with a black box. If no allele of corresponding size was found in
 212 the list of Frenkel et al., 2012 a ‘?’ was inserted.

	EmMS-01	EmMS-02	EmMS-03	EmMS-04	EmMS-05	EmMS-06	EmMS-07	EmMS-08	EmMS-09	EmMS-10	EmMS-11
Allele	219	168	218	290	167	249	177	185	155	251	171
EU-Isolate	A+B	B	B	B?	A+B	B?	B	B	A+B	A+B	B
Frenkel et al, 2012	239	185	236	305/?	186	266/?	195	205	176	271	191
Frenkel et al, M13 adj.	220	166	217	286/?	167	247/?	176	186	157	252	172

213
 214 To test the aggressiveness of this isolate, inoculations with *in vitro* plants of
 215 ‘Regent’ and ‘Chardonnay’ were performed. Samples were taken one, four, five and
 216 15 days past inoculation with day one providing the reference for the latter. The
 217 increase of fungal biomass could be observed for both genotypes. At four dpi a
 218 significant difference between ‘Regent’ and ‘Chardonnay’ was observable which was
 219 absent at 5 dpi. After 15 days a clear difference between ‘Regent’ and ‘Chardonnay’
 220 was observed with ‘Chardonnay’ showing a median fold change of approximately 65
 221 compared to a fold change of around 20 for ‘Regent’ (Figure 3, A).



222

223 Figure 3: Characterization of PM isolate GF.En-01. **A** Fungal biomass increase over time as measured
 224 by qPCR for 'Chardonnay' and 'Regent'. **B** Staining of leaves one day past inoculation with
 225 Diaminobenzidin and Calcofluor-White (gs = germinated spore, hy = hyphae, ap = appressoria, pen
 226 = penetration site). **C** Counting of conidiospores one day past inoculation and grouping them
 227 according to different developmental stages.

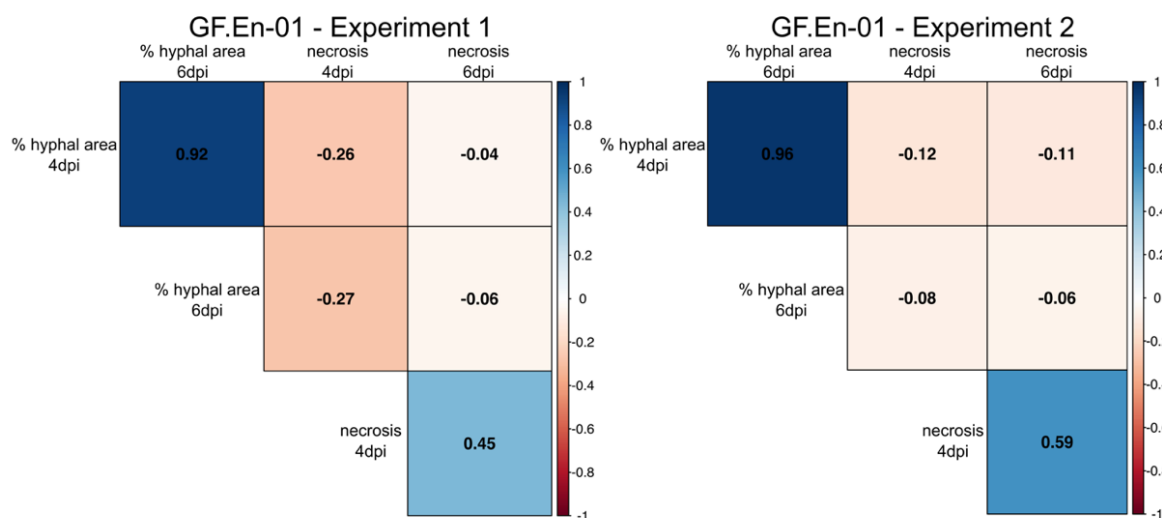
228 In addition, at one day after inoculation, the leaf discs were stained with
 229 Diaminobenzidin (DAB) and Calcofluor-White (CW). The DAB stain visualizes
 230 reactive oxygen species (ROS) by forming a brown stain at sites with elevated ROS
 231 levels. The CW stain visualizes the transparent conidiospores and hyphae. A clear
 232 accumulation of ROS was observable at the penetration site of the appressoria in
 233 'Regent'. The brown DAB stain extended around the cell in the appoplast. This
 234 reaction was much less pronounced and restricted to the actual penetration site in
 235 the susceptible 'Chardonnay'. Furthermore, primary and secondary hyphae were
 236 observed on susceptible 'Chardonnay' leaves (Figure 3, B).

237 During staining spores were counted and grouped according to different
 238 developmental stages. The major difference between the susceptible 'Chardonnay'
 239 and the resistant 'Regent' was the overall germination rate, which was 97 % in
 240 'Chardonnay' versus 62 % on 'Regent'. On 'Regent' leaves, a big portion of

241 germinated spores showed only germ tubes at one day past inoculation (Figure 4).
242 On 'Chardonnay' most of the spores germinated and successfully formed
243 appressoria. No papilla formation was detectable for the biggest proportion of spores
244 (Figure 3, C, ~60 %). On 'Regent' the larger portion of germinated spores were
245 accompanied by papilla formation (Figure 3, C, ~30 %). Taken together, these
246 results indicate that *Ren3/Ren9* is capable of restricting the growth of the GF.En-01
247 isolate. Studying the two resistances independently should therefore be possible
248 with this isolate. However, it indicates that *Ren3/Ren9* mediates only a partial PM
249 resistance against this *E. necator* EU-B type isolate.

250 2.5 Leaf disc infection assays with GF.En-01

251 Two independent inoculation experiments were performed with the single spore
252 PM isolate GF.En-01. Datasets for hyphal growth and necrosis formation from both
253 experiments were compared with each other in a correlation plot. In previous studies
254 a hypersensitive response (HR) / necrosis associated with the appressoria of PM
255 has been proposed as a mechanism for *Ren3* and *Ren9* mediated resistance [15].



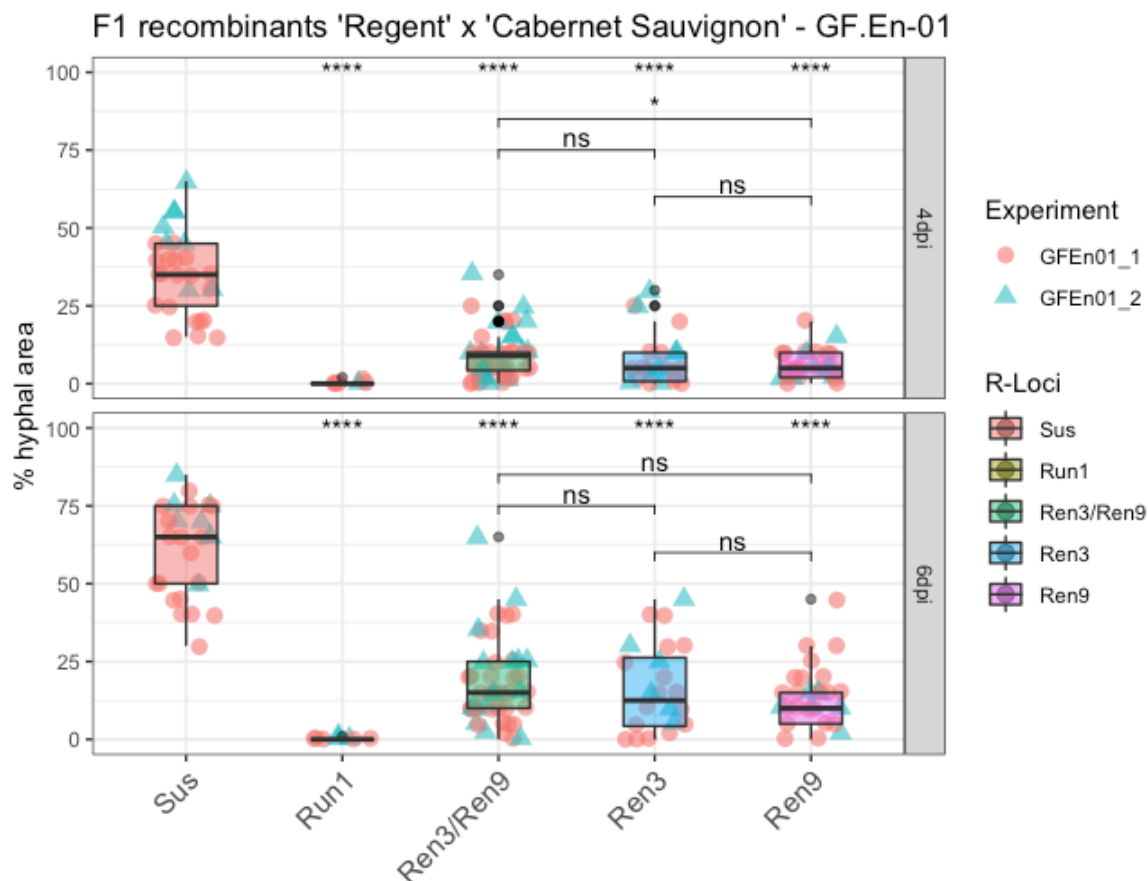
256

257 Figure 4: Correlation plot of the percentages of hyphal area and necrosis formation at 4 and 6 dpi.
258 Positive correlations are indicated in blue and negative correlations are indicated with red. The data
259 is split into the two independent experiments. (Significance level: $p < 0.05$; all correlations were
260 significant)

261 Here, a significant positive correlation was observed for percentage of hyphal
262 area present at 4 and 6 dpi comparing both experiments (Figure 4). In addition, a
263 strong positive correlation for necrosis formation was observed for 4 and 6 dpi in
264 both experiments (Figure 4). Percentage of hyphal area showed in all cases a
265 negative correlation with necrosis formation. The strongest negative correlation was

266 observed in both experiments at 4 dpi (Figure 4), indicating a small negative effect
267 of necrosis formation on hyphal growth. Six days past inoculation only a very weak
268 negative correlation was found between these two scored traits (Figure 4).

269



270

271 Figure 5: Boxplots of percentage of hyphal area at four (4dpi) and six days past inoculation (6dpi). F1
272 individuals with the same R-locus combination were grouped. Phenotypic scores from different
273 experiments are indicated by different shapes and colors of the data points. Outliers were colored in
274 black. Mean of respective groups are compared to the susceptible group and the mean of the different
275 *Ren3* and *Ren9* combinations with each other (**** = $P \leq 0.0001$, *** = $P \leq 0.001$, ** = $P \leq 0.01$, * = P
276 ≤ 0.05 , NS = not significant $P > 0.05$).

277

278 After a global analysis of the datasets an analysis of the different R-loci
279 combinations was performed by grouping the phenotypic scores of F1 individuals
280 from the 'Regent' x 'Cabernet Sauvignon' cross with similar combinations. As
281 controls, a breeding line with the strong PM resistance locus Run1 and the PM
282 susceptible genotypes 'Cabernet Sauvignon', 'Chardonnay' (experiment 1,
283 GFE01_1) and 'Diana' (experiment 2, GFE01_2) were added in the experiments
284 (Figure 5, Sus, Run1). Means of the different R-loci combinations were compared to
285 the susceptible group to detect statistical differences. For all groups a significant

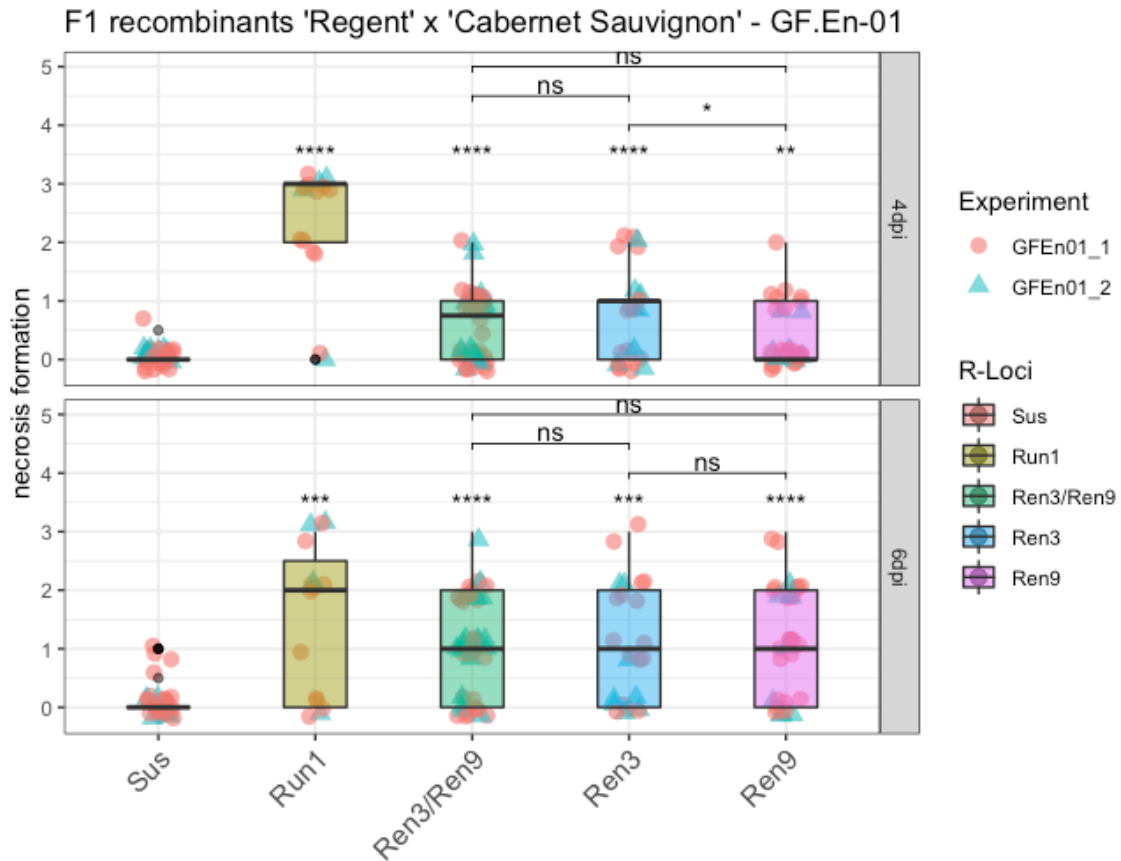
286 difference to the susceptible control could be observed at four- and six-days past
287 inoculation (Figure 5). For *Run1*, a strong HR was observed associated with the
288 primary appressoria of the conidiospores of GF.En-01, as already well documented
289 in several studies [18–20](Figure S2). This HR prevented any growth of PM on leaf
290 discs of this genotype (Figure 5, *Run1*). In contrast to that, individuals with the
291 different *Ren3* and *Ren9* combinations showed variable resistance to PM.
292 Phenotypic scores of *Ren3/Ren9* individuals showed the highest variation and were
293 overlapping four- and six-days past inoculation with those of the susceptible control
294 group (Figure 5).

295 However, the median of percentage hyphal area of the *Ren3/Ren9* group
296 increases from approximately 12 % to roughly 18 %, which is a clear difference
297 compared to the ~35 % to ~65 % change of the susceptible group (Figure 8). To test
298 if there is any significant difference between “*Ren3-only*” or “*Ren9-only*” and the
299 combination of both resistance loci, the means of these groups were compared. Only
300 at 4 dpi a significant lower percentage of hyphal area was observed for “*Ren9-only*”
301 compared to “*Ren3/Ren9*” (Figure 5). After six days, no significant differences were
302 observed between the three groups (Figure 5).

303 In addition to percentage hyphal area, the trait necrosis formation was scored.
304 The phenotypic data was analyzed the same way as percentage of hyphal area.
305 Necrosis formation of the different *R*-loci combination carriers was compared to the
306 susceptible control group. At both four- and six-days past inoculation the grapevines
307 with the various *R*-loci combinations showed a significant difference compared to the
308 susceptible group (Figure 6).

309 The breeding line with *Run1* showed, as already described, a strong HR
310 associated with nearly all primary appressoria formed by the conidiospores, which is
311 indicated by a median score of three and two at 4 dpi and 6 dpi (Figure 6, *Run1*).
312 Median scores of *Ren3/Ren9* and “*Ren3-only*” were around one at 4 dpi, whereas
313 *Ren9* showed a median score of zero at 4dpi, a significant difference compared to
314 *Ren3/Ren9* (Figure 6). At 6 dpi the different combinations of *Ren3* and *Ren9* all
315 showed a median score of one but overall the scores were ranging from zero to 3
316 (Figure 6).

317



318

319

320

321

322

323

324

Figure 6: Boxplots of necrosis formation associated with appressoria at four (4dpi) and six days past inoculation (6dpi). F1 individuals with the same R-locus combinations were grouped. Phenotypic scores from different experiments are indicated by different shapes and colors of the data points. Outliers were colored in black. Mean of respective groups are compared to the susceptible group and the mean of the different Ren3 and Ren9 combinations with each other (**** = $P \leq 0.0001$, *** = $P \leq 0.001$, ** = $P \leq 0.01$, * = $P \leq 0.05$, NS = not significant $P > 0.05$).

325

326

327

328

329

330

331

332

333

334

335

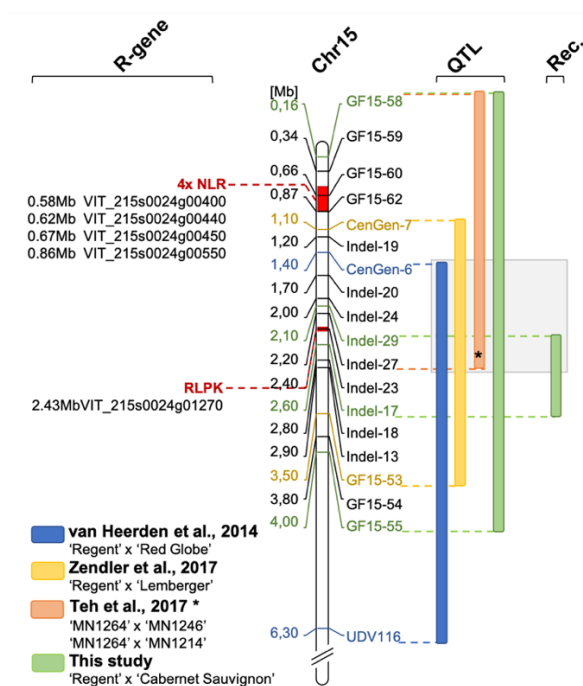
336

337

3. Discussion

Several studies reported a shift of the QTL for resistance to PM on chromosome 15. Van Heerden et al., 2014 showed a LOD_{max} marker CenGen-6 associated with resistance to PM which is located at 1.4 Mb, and a total interval from CenGen-6 to UDV-116 on chromosome 15 (Figure 7, blue bar). In another study, the same research team showed the *Ren3* QTL associated with marker UDV-116, which is located in the middle of chromosome 15. One could argue that, if the marker density in the anterior part of chromosome 15 would have been increased, the QTL would have been possibly shifted further to the beginning of the chromosome [21]. Teh et al. [22] also investigated the resistance *Ren3* with a SNP based genetic map and phenotypic field data. Their interval for resistance to PM ranged from 0.09 to 2.2 Mb on chromosome 15 (Figure 7, orange bar).

350



351

Figure 7: Overview of QTLs for resistance to PM in the anterior part of chromosome 15. Bars next to the map of chromosome 15 indicate QTL intervals ($LOD_{max} \pm 1$). Physical positions are presented in respect to the reference genome of PN40024 12x v2 using the position of the genetic markers applied in this study. The QTL revealed in this study (green bar) represents the largest observed interval in the front part of chromosome 15 (enclosing the results of 16-2, -3 and -4). In addition, the interval resulting from the analysis of F_1 individuals with meiotic recombination on chromosome 15 is indicated (Rec.). The overlap of all four QTL analyses is highlighted in grey. The region from the start of the chromosome to the position of marker GF15-55 was searched for resistance gene analogs (R-gene, NLR = Nucleotide binding leucine rich repeat, RLPK = receptor like protein kinase). Possible regions are indicated in red. (* The physical position of the QTL interval of Teh et al. [22] was approximated to physical positions of markers in this study according to SNP positions in their supplemental material)

363

364 In a previous study for the delimitation of the resistance locus *Ren3*, a second
365 resistance associated region was identified on chromosome 15. This region, now
366 termed *Ren9*, was located in the front part of chromosome 15 and mediated necrosis
367 associated with the appressoria of PM nine days past inoculation [15]. The region of
368 this resistance locus could be delimited to a 2.4 Mb interval flanked by the genetic
369 markers CenGen-7 and GF15-53 (Figure 7, yellow bar) [15].

370

371 **3.1 QTL analysis**

372 In the study presented here a QTL analysis was performed with the previously
373 published genetic map of 'Regent' x 'Cabernet Sauvignon' [15] and new phenotypic
374 data for resistance to PM. The progression of the infections was scored at four dates
375 during the viticulture season in 2016. Analysis after grouping the individuals into their
376 respective R-loci combinations (susceptible, *Ren3*, *Ren9*, *Ren3/Ren9*) indicates a
377 significant difference between the carriers of *Ren3/Ren9* and the susceptible group.
378 At all four scoring dates there is clear evidence for a positive effect of the two R-loci
379 on the inhibition of PM growth (Figure 1). In the beginning of the season, the
380 phenotypes of the majority of the genotypes were shifted towards resistance (Figure
381 1, 16-1). The QTL results for this date show a QTL-region flanked by the markers
382 UDV-116/GF15-30 and GF15-42/ScOR-A7 (Figure 2). This region agrees with the
383 previously published localization of locus *Ren3* [15,21] and confirms it in this
384 independent mapping study. The phenotypic scores of genotypes without any R-
385 locus are shifted towards susceptible (9) from the second scoring date onwards
386 (Figure 1, 16-2 to 16-4) reflecting the developing PM epidemic and increasing
387 infection pressure. The two individuals with only *Ren3* showed a median phenotypic
388 score alike or higher than the susceptible genotypes at the later scoring dates (16-
389 2, 16-3, Figure 1). QTL analysis for the dates 16-2, 16-3 and 16-4 revealed a QTL
390 shift towards the anterior end of chromosome 15 (Figure 2). The flanking markers
391 for the QTLs of dates 16-2 and 16-3 are GF15-62 and CenGen6/CenGen7 (Figure
392 2, Tab. 1). The LOD_{max} marker in both cases is CenGen6 with a LOD score of 39.5
393 – 45 explaining 58.6 – 63.8 % of phenotypic variance (Figure 2, Tab. 1). This result
394 agrees with the finding of van Heerden et al. [23], who identified CenGen6 as the left
395 flanking genetic marker in their QTL analysis for PM resistance. QTL analysis with
396 the cross 'Regent' x 'Lemberger' also had indicated high LOD scores for markers in
397 the anterior part of chromosome 15 for the sampling dates 2015-1, 2015-2 and 2016-

398 1 [15]. The interval mapping of these three dates revealed GF15-10 and CenGen-6
399 as left flanking genetic markers [15].

400 The scoring date 16-4 was at the very end of the season and the epidemic. At
401 this time, a strong infection pressure should have been built up resulting in a shift of
402 the phenotypic scores towards susceptibility for all carriers of R-loci (Figure 1). Yet,
403 *Ren3/Ren9* carrying individuals show a median score of 3 and most of the individuals
404 range from 1 – 5 at this time of the season (Figure 2). The QTL analysis with this
405 dataset shows reduced LOD scores for all markers. The QTL region, however, is still
406 associated with the anterior region of chromosome 15. The LOD_{max} marker is GF15-
407 62, indicating a further shift of the QTL region to the beginning of chromosome 15,
408 in agreement with the findings of Teh et al. [22] (Figure 2, Table 1). This marker still
409 explains about 38 % of the observed variance (Table 1). Taken together, these
410 results from four independent grapevine crosses show a high likelihood of *Ren9*
411 being located in the front part of chromosome 15 at around 0 to 4Mb (Figure 7). The
412 region of overlap between all four QTLs ranges from 1.4 to 2.0 Mb defining it as a
413 high confidence area (Figure 7).

414 Additionally, the new QTL analysis presented here underscores the fact that the
415 loci *Ren3/Ren9* mediate partial- but not total-resistance against powdery mildew.

416 **3.2 Fine mapping of the *Ren9* region**

417 Detailed investigations were carried out with a subset of individuals exhibiting
418 meiotic recombinations on chromosome 15 that separate the two resistance loci
419 *Ren3* and *Ren9* (Table 2). Newly designed insertion / deletion markers (Indel) are
420 highlighted by a black square around them (Table 2, Table S1). The OIV455 field
421 scores from 2016 are shown and the average was calculated (Table 2). Individuals
422 with the same R-loci combination were grouped and their phenotypic score was
423 averaged. The combined resistance *Ren3/Ren9* or “*Ren9*-only” show an average
424 field score of ~1.2 to ~2 whereas two individuals with “*Ren3*-only” showed an
425 average score of 5.5 (Table 2). One possible explanation for these results might be
426 that during the season in 2016 a change of the composition of PM isolates took
427 place. Isolates that are more virulent may emerge at the end of the season and could
428 be capable of breaking *Ren3*. For Europe two dominant PM isolates have been
429 described termed EU-A and -B [17]. Recent studies on PM isolates in vineyards in
430 Hungary have shown EU-B to be the first isolate in the season sampled on flag-
431 shoots. Later during the season in summer and autumn a mixture of EU-B, -B2 and

432 -A was detectable [24]. Similar events may happen in the vineyards around the
433 Institute for Grapevine Breeding Geilweilerhof, Germany and would explain the
434 results for these F₁ individuals.

435 However, one individual (1999-074-239) which was previously classified as
436 “*Ren3*-only” showed an OIV455 score of 1 throughout the season (Table 2). For
437 genetic map construction only GF15-53 (3.5 Mb) and CenGen-7 (1.1 Mb) were
438 available as reliable genetic markers to assess recombination points in this genetic
439 area. For fine mapping of the recombination points, new genetic Indel markers were
440 developed in this study (Table 2, Indel, Table S1). These new genetic markers further
441 defined the recombination points for the individuals 1999-074-239, -204 and -136
442 (Table 2). For the F₁ individuals 1999-074-136 and 1999-074-204 the recombination
443 point from susceptible to resistant was located between the markers Indel-17 (2.6
444 Mb) to Indel-13 (2.9 Mb). For the genotype 1999-074-239 the recombination
445 happened between Indel-29 (2.1 Mb) and Indel-27 (2.2 Mb).

446 As the phenotypic scores of 1999-074-239 are similar to those of *Ren3/Ren9*
447 and “*Ren9*-only” (Table 2, average OIV score of *Ren9* = 1.2 and *Ren3/Ren9* = 2) we
448 hypothesize that this individual is carrying both resistances. This would mean that
449 the interval between Indel-29 and Indel-13 (2.1 – 2.9 Mb) could represent the *Ren9*
450 encoding region and delimit this resistance locus to around 0.8 Mb. For breeders this
451 result means a much smaller introgression required to gain resistance and removal
452 of possible genetic drag. The Indel markers designed here can easily be applied for
453 marker-assisted selection in new breeding programs for stacking multiple
454 resistances in novel grapevine cultivars improved in fungal resistance.

455 The average OIV scores for the different *R-locus* combinations suggests that
456 under field conditions of the year 2016 *Ren9* was the major resistance against PM.
457 Average OIV scores of 1.2 for “*Ren9*-only” individuals and 2 for *Ren3/Ren9* plants
458 clearly differ from “*Ren3*-only” carriers with an average score of 5.5 (Table 2).
459 However, in a study published by an Italian research team *Ren9* carrying genotypes
460 exhibited a reduced level of resistance against PM in unsprayed fields in Italy
461 compared to “*Ren3*-only” and *Ren3/Ren9* individuals [25]. This may indicate a
462 different composition of PM isolates in the fields of Germany and Italy with different
463 virulence levels breaking either the resistances encoded by *Ren3* or *Ren9*. However,
464 this hypothesis should be treated with care. In the study presented here, the number
465 of individuals investigated was limited and the observations were only for one year.

466 Further research with more individuals carrying the different *R*-locus combinations
467 over several years is required to elucidate this observation in more detail.

468 **3.3 Leaf disc inoculation**

469 The individuals from Table 2 were submitted to artificial inoculation experiments
470 with a single spore isolate sampled in the field of the JKI, Institute for Grapevine
471 Breeding Geilweilerhof, Germany. The PM isolate GF.En-01 was genotyped with the
472 published SSR markers [17]. The allele combinations obtained from the genotyping
473 indicate that this isolate represents most likely the EU-B type (with some uncertainty
474 remaining for the markers EnMS-04 and -06). This divergence can be explained by
475 the limited precision of capillary electrophoresis and the use of fluorescent dyes that
476 might slightly change the apparent size of amplicons. Further, it was necessary to
477 adapt the published sizes of Frenkel et al. [17] by subtracting the 19 bp of the M13
478 sequencing tag they used from the amplicon sizes obtained in capillary
479 electrophoresis.

480 Growth of GF.En-01 was significantly reduced on ‘Regent’ compared to the
481 susceptible genotype ‘Chardonnay’ (Figure 3, A). There is clear evidence that the
482 development was much slower on *Ren3/Ren9* compared to the susceptible control
483 (Figure 3, C). The inhibition of growth was most likely due to the establishment of
484 papilla and ROS at sites of penetration (Figure 4, B). These are typical resistance
485 responses against grapevine powdery mildew [13].

486 After this characterization, GF.En-01 was used for leaf disc inoculation
487 experiments of the recombinant F_1 individuals from Table 2. Two independent
488 inoculation experiments were performed yielding similar results. The data for the two
489 traits percentage of hyphal area and necrosis formation were tested for correlation
490 to investigate a possible effect of necrosis formation on hyphal growth. In the two
491 independent experiments a weak, yet significant negative correlation between
492 necrosis formation and hyphal growth could be observed at four days past
493 inoculation. This trend was much weaker six days past inoculation (Figure 4).
494 However, these findings indicate that there is indeed an interaction between these
495 traits showing that necrosis formation contributes to some small extent to the
496 inhibition of PM growth.

497 To investigate the effects of the different *R*-loci combinations in detail, the
498 phenotypic scores of the individuals with similar *R*-loci were grouped. This grouping
499 showed that there is no significant difference between the respective *Ren3* and *Ren9*

500 combinations in terms of percentage of hyphal area covering the leaf discs except
501 at four dpi in the comparison of *Ren3/Ren9* to “*Ren9-only*”. These two showed a
502 significant difference with *Ren9* showing less hyphal growth. Most of the phenotypic
503 scores are overlapping between *Ren3/Ren9* and “*Ren3-only*” making this difference
504 marginal. Nevertheless, for all *R*-loci combinations a significant reduction in hyphal
505 growth compared to the susceptible controls could be observed at both four- and six-
506 days past inoculation (Figure 5). These results indicate that both resistance loci by
507 themselves are capable to detect the EU-B PM isolate and inhibit its growth. It also
508 shows that both resistances are equally strong and no additive effect can be
509 observed when stacking them, at least when dealing with this specific single spore
510 isolate.

511 The trait necrosis formation was investigated the same way. The *R*-loci
512 combinations of *Ren3* and *Ren9* showed at both dates a significant difference
513 compared to the susceptible controls. A significant difference among the
514 combinations for “*Ren3-only*” compared to “*Ren9-only*” at four days past inoculation
515 was also shown (Figure 7). This might indicate that the mechanism behind the two
516 resistances differs in terms of detection speed. This difference cannot be observed
517 anymore at six days past inoculation. Trailing necrosis, as it was observed for PM
518 on leaves, is described as a part of ontogenetic resistance of grapevine berries of
519 ‘Chardonnay’ [26,27]. However, all artificial inoculation experiments were performed
520 with young and healthy leaves from the shoot tip and trailing necrosis was absent on
521 the susceptible control leaves from ‘Cabernet Sauvignon’, ‘Chardonnay’ and ‘Diana’.
522 These results indicate that the mechanism observed here differs from the one
523 described for ontogenetically resistant grape berries. Therefore, we propose that the
524 resistance of *Ren3* and *Ren9* relies on a faster detection of PM pointing at specific
525 R-gene interactions.

526 **3.4 Possible candidate genes**

527 The resistances *Ren3* and *Ren9* although partial, might rely on different
528 mechanisms. The resistance-associated region for *Ren3* was searched for
529 candidate genes. This yielded a cluster of four NLR genes in the reference genome
530 [15]. Screening the reference genome of PN40024 12x V2 in the proposed QTL
531 interval for *Ren9* yielded two regions with R-gene analogs. The first region, at the
532 very beginning between 0.5 and 0.9 Mb of chromosome 15, comprises a cluster of
533 four possible NLR genes (Figure 7, 4xNLR) and is supported by QTLs from this study

534 and the study of Teh et al. [22]. This cluster might look different in the genome of
535 resistant 'Regent'. It therefore is of high interest for further investigations. NLR genes
536 have been proven to be key-players in several plant resistance reactions against a
537 multitude of different pathogens [28,29]. Furthermore, the well characterized
538 resistance locus *Run1* which was used in this study as a positive control for
539 resistance against PM was shown to rely on a NLR gene of the "Toll-Interleukin-
540 Receptor-like" type [19].

541 The second region with another *R*-gene analog is found around 2.4 Mb in a
542 region where multiple QTLs from different crosses overlap ([15,23] and this study). In
543 addition to the QTL intervals, the recombination-points of the F₁ individuals 1999-
544 074-239 and 1999-074-204 point to this region (Figure 7). The gene found here
545 shows the typical functional domains of a leucine-rich-repeat receptor-like protein-
546 kinase. Such functions are important for the detection of pathogen associated
547 molecular patterns (PAMPs). One of the most prominent examples of PAMP
548 triggered immunity (PTI) is the detection of flagellin by the receptor-like protein-
549 kinase BAK1 in a complex with other receptor like kinases [30]. Roughly 872 of
550 receptor-like kinases are encoded in the grapevine genome [31]. However, any
551 important role of the RLK gene in PM resistance has to be confirmed by functional
552 studies. Therefore, transformations of susceptible cultivars with the possible
553 candidate genes have to be performed and knock-out / -down experiments with
554 resistant cultivars carrying *Ren9* are required. If the RLK gene would prove to be the
555 important one this could indicate that the pathogen perception mediated by *Ren3*
556 and *Ren9* most likely differs between the two. This in turn would be most interesting
557 for breeders. A combination of different resistance mechanisms in pyramiding
558 resistance loci is most promising to generate long-term durability.

559

560

561

562

563

564

565

566

567

568 **4. Materials and Methods**

569 **4.1 Plant material**

570 Progeny used for genetic mapping comprised 236 F₁ individuals from the cross
571 of 'Regent' x 'Cabernet Sauvignon'. The plants of this population are grown in the
572 experimental fields at JKI Geilweilerhof, Siebeldingen, Germany (49°12'54.1"N
573 8°02'41.3"E) on their own roots with a spacing of 1.8 to 1.1 m (row by vine). They
574 are cane pruned as is common practice in this wine growing area (Palatinate region).
575 The plantation density at JKI Geilweilerhof, Siebeldingen, is 5050 vines per hectare.
576 The 'Regent' x 'Cabernet Sauvignon' progeny is maintained in an experimental
577 vineyard that was left unsprayed with fungicides. All of the 236 genotypes are
578 represented by one plant each.

579 For inoculation experiments, plants were kept in the greenhouse as two eye
580 cuttings. Plants were treated with Sulphur once per week to prevent PM infection.
581 One week prior to inoculation experiments plants were not sprayed anymore and the
582 third fully expanded leaf, counting from the shoot tip, was sampled.

583 *In vitro* plants for artificial inoculation experiments were contained on MS233
584 (Duchefa, 2.3 g/l) with sucrose (0.11M) and gelrite (0.5 % (w/v), pH 5.8) media.
585 Plants were propagated every 12 weeks by two eye cuttings and were kept in climate
586 chambers with 16 hours light, 8 hours dark and 20 – 22 °C.

587 **4.2 Powdery mildew**

588 For controlled inoculation experiments, a single spore isolate was collected from
589 'Lemberger', a susceptible grapevine cultivar grown in the fields of the Institute. The
590 isolate was propagated every three to four weeks on surface sterilized 'Chardonnay'
591 leaves maintained on 1% water agar. The inoculated leaves were incubated under
592 long day conditions (16h light, 8h dark). Temperatures were set to 23°C during the
593 day and to 19°C during the night.

594 **4.3 DNA extraction**

595 For DNA extraction, about 1cm² pieces of young and healthy leaves were
596 collected from the field and the greenhouse plants, transferred in plastic bags and
597 immediately cooled on ice upon transfer to the laboratory. Leaf segments were
598 shock-frozen in liquid nitrogen and stored at -70°C. DNA was extracted after grinding
599 the samples in the frozen state with a tissue lyser mill (Retsch, 42781 Haan,
600 Germany) using the Macherey Nagel (52355 Düren, Germany) Nucleospin 96 II DNA

601 kit or the PeqGOLD Plant DNA mini Kit (PEQLAB GmbH, 91052 Erlangen, Germany)
602 as described in [14].

603 **4.4 Genetic marker design around Ren9**

604 For the development of insertion / deletion (Indel) markers in the *Ren9* region,
605 the reference genome PN40024 12x.v2 [32,33] was used. Genetic marker
606 development was performed as described in Zendler et al. [15]. Sequences showing
607 length polymorphisms greater than six bp were tested for PCR amplification. Unique
608 flanking oligonucleotides for PCR amplification of polymorphic regions were selected
609 according to standard conditions (~50% GC content, 20 – 25 bp lengths, T_a 55 -
610 60°C). PCR reactions were performed in a 10µl reaction mix using the Kapa 2G
611 Multiplex Mix (PeqLAB GmbH, 91052 Erlangen, Germany). PCR products were
612 analyzed on 3% agarose gels with Serva Clear Stain.

613 **4.5 SSR-marker analysis**

614 The construction of genetic maps employed SSR markers. SSR marker analysis
615 was performed in multiplex PCR assays with the Kappa2G Multiplex Kit (PeqLAB
616 GmbH, 91052 Erlangen, Germany) mixing up to five different oligonucleotide pairs
617 in one PCR. The forward primer of each pair was 5'- end labeled with fluorescent
618 dyes HEX®, ROX®, FAM® or TAMRA®. Allele sizes were analyzed using the
619 ABI3130XL sequencer with a 36 cm capillary set, a size standard labeled with LIZ®
620 (identical to GeneScan™ 500 LIZ™, Applied Biosystems™) and GeneMapper® 5.0
621 software (Applied Biosystems™) [15].

622 **4.6 Construction of the genetic map**

623 Genetic maps of chromosome 15 were constructed by linkage/recombination
624 analysis using JoinMap®4.1 software [34]. Allele combinations observed in the SSR
625 marker data were encoded according to the manual of JoinMap®4.1. Grouping was
626 done using the independence LOD parameter starting at LOD 2.0 up to LOD 10.
627 Maps were calculated using the Maximum Likelihood mapping algorithm provided in
628 the JoinMap®4.1 software. For 'Regent' x 'Cabernet Sauvignon' the previously
629 published integrated and maternal/paternal genetic maps were used [15]. Individuals
630 which were accidentally selfed or had more than 30% missing data for the analyzed
631 genetic markers were excluded from the mapping calculation to avoid erroneous
632 marker order. Final analysis was based on 236 F1 individuals from the cross of
633 'Regent' x 'Cabernet Sauvignon'.

634 **4.7 Phenotypic data**

635 4.7.1 Phenotypic field data

636 Phenotypic data for QTL analysis was obtained from evaluation of field plants
637 under natural infection pressure with *E. necator*. In former years, resistance scores
638 had been collected once a year in late summer (end of August to end of September)
639 following the inverse OIV (International Organisation of Vine and Wine,
640 <http://www.oiv.int>) classification as described [14]. In the year 2016, individuals of
641 the cross 'Regent' x 'Cabernet Sauvignon' were scored four times every three to four
642 weeks (26-06-16 *E.n.*-leaf-16-1, 29-07-16 *E.n.*-leaf-16-2, 18-08-16 *E.n.*-leaf-16-3,
643 12-10-16 *E.n.*-leaf-16-4). The degree of infection was classified in grades of 1, 3, 5,
644 7 and 9 (1=no infection at all, 3=nearly no infection visible, 5=punctual infection spots
645 on several leaves, 7=punctual infection on every leaf, 9=infections covering all
646 leaves) (inverse to OIV descriptor 455). Each phenotypic scoring was performed by
647 two people. Scores were assigned by visual inspection of the whole plant.

648 4.7.2 Artificial inoculation experiments using in vitro plants

649 For characterization of the *E. necator* single spore isolate GF.En-01, controlled
650 inoculation experiments with *in vitro* plants of 'Regent' and 'Chardonnay' were
651 performed. Leaves were placed on 1% water agar and inoculated with a brush. Fresh
652 conidiospores were taken from infected 'Chardonnay' leaves as described above.
653 To characterize the development of the isolate over time, biomass increase was
654 measured by qPCR [35]. Samples were taken at one-, four-, five- and 15 days past
655 inoculation. A fold change was calculated with the delta-delta c_t method, using one
656 dpi as normalization point. Detailed characterization employed Diaminobenzidin
657 (DAB) and Calcofluor-White (CW) staining one day past inoculation. Leaves were
658 first stained by DAB according to a published protocol [36] and then exposed to
659 Calcofluor-White. As the leaves of *in vitro* plants were very tender, the incubation
660 time with DAB was reduced to two hours. For CW staining, leaves were treated
661 according to the manufacturers instructions with one drop of CW staining solution
662 and an equal drop of 10% KOH (Fluka chemicals). The samples were incubated for
663 one minute and then washed with sterile water. Microscopy was performed directly
664 after Calcofluor-White staining. At this point, spores were counted and grouped
665 according to their different developmental stages. For each genotype, three times
666 100 spores were counted from three independent leaves.

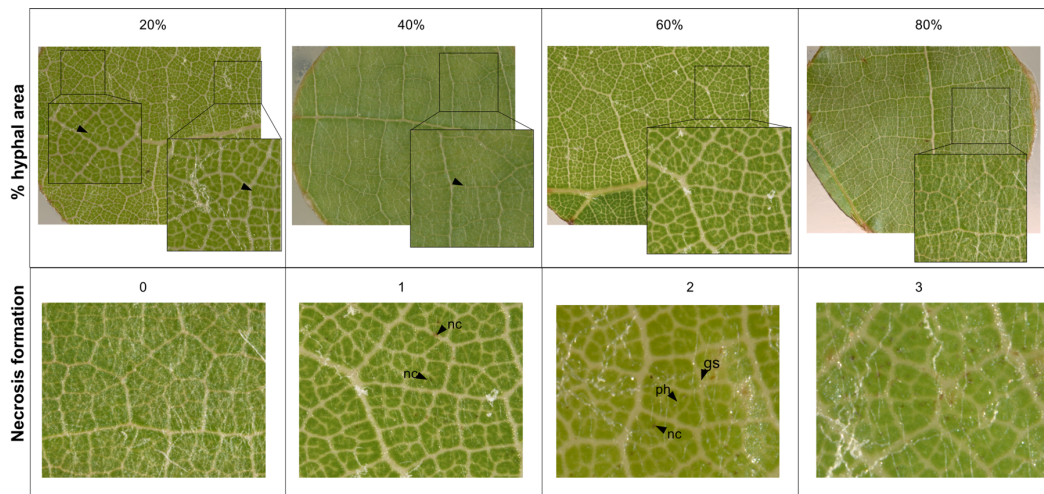
667 4.7.3 Experimental leaf disc inoculation experiments

668 For detailed investigations of selected recombinants from the 'Regent' x
669 'Cabernet Sauvignon' cross artificial inoculations of leaf discs were carried out as
670 described in [37]. In total, four leaf-discs per genotype from four different plants were
671 placed on 1% water agar plates. They were inoculated with a spore suspension of
672 an *Erysiphe necator* isolate originating from a susceptible 'Lemberger' plant in the
673 field.

674 The PM isolate GF.En-01 was cultivated on leaves of the susceptible cultivar
675 'Chardonnay'. Around 10 to 15 days prior to the inoculation experiment six leaves
676 from 'Chardonnay' were surface sterilized in 1:10 diluted bleach solution (Eau de
677 Javel, 100ml solution containing 2.6g NaClO) for two minutes. Leaves were rinsed
678 three times with deionized water and dried between paper towels before they were
679 placed in Petri dishes containing 1% water agar. Leaves were then inoculated using
680 10 to 15 single spore chains of GF.En-01. Leaves for the inoculation experiment
681 were surface sterilized in the same way before punching discs with a one cm
682 diameter cork-borer. The day after placing the leaf discs on 1% water agar the spore
683 suspension was prepared by shaking the inoculated 'Chardonnay' leaves in 15 ml
684 sterile water with 10 µl Tween-20. Spores were counted using a hemocytometer.
685 Spore suspensions with $1 \times 10^5 - 2 \times 10^5$ spores/ml were used for inoculation with a
686 pump sprayer. Visual inspection ascertained that all leaf discs were covered equally
687 with the spore suspension. As a control the cross parental types 'Regent' and
688 'Cabernet Sauvignon' were included together with the susceptible cultivar
689 'Chardonnay' or 'Diana' as well as a breeding line that carries the strong PM
690 resistance locus *Run1* (VRH3082-1-42).

691 Leaf disc scoring was performed at four- and six-days past inoculation. The
692 percentage of leaf disc area covered by hyphae and necrosis formation was scored
693 visually using a stereo microscope (Zeiss Axiozoom V16).

694



695

696

697

Figure 8: Examples for visual scoring of percentage of hyphal area- and necrosis (gs = germinated spore, ph = primary hyphae, nc = necrosis)

698

699

700

701

702

703

704

705

Necrosis formation associated with appressoria was scored on a scale of 0 to 3: 0 = no necrosis, 1 = random necrosis associated with appressoria, 2 = trailing necrosis at primary hyphae, 3 = necrosis associated with nearly all appressoria formed by PM (Figure 8). Phenotypic data was analyzed and visualized with R [38] and the packages `ggpubr` (`stat_compare_means()`) [39]. Correlations were calculated using the `cor()` and `cor.mtest()` package (`method = "spearman"`) and visualized with the package `corrplot()` of R [40]. Code and data for reproduction of graphs can be found in the supplemental material (Table S2 – S4).

706

4.8 QTL-analysis

707

708

709

710

711

712

713

714

715

716

717

718

719

QTL analysis was performed using MapQTL®6.0 software [41] with standard settings on the integrated and parental maps. The dataset for the separate parental maps was re-coded as doubled haploid population as recommended in the MapQTL®6 manual to avoid “Singularity errors” [41] and enable downstream QTL analysis. The improved maternal genetic map of ‘Regent’ and the paternal genetic map of ‘Cabernet Sauvignon’ were combined with the phenotypic data from the field. Interval mapping (IM) and multiple QTL mapping (MQM) with automatic co-factor selection were performed with the datasets *E.n.-leaf-16-1*, *E.n.-leaf-16-2*, *E.n.-leaf-16-3* and *E.n.-leaf-16-4*. A permutation test with 1000 permutations determined the linkage group (LG) specific significance threshold for each trait at $p \leq 0.05$.

720 **5. Conclusions**

721 Both analyses from field and laboratory show that the resistance loci *Ren3* and
722 *Ren9* mediate partial resistance to PM. In generating new breeding lines for
723 European viticulture, *Ren3* and *Ren9* should be complemented by strong resistance
724 loci such as *Run1*, which completely inhibits the progression of the isolate GF.En-01
725 (representing the EU-B type of powdery mildew). The resistance loci *Ren3* and *Ren9*
726 are broken in Eastern North American vineyards as shown by inoculation
727 experiments with NY19, an PM isolate sampled from vineyards in New York, USA
728 [22]. In controlled inoculation experiments with this isolate Teh and collaborators [22]
729 could not reproduce the QTL from field data for *Ren3/Ren9*. A similar fate might
730 await these resistance loci at some point in Europe, as the evolution of the pathogen
731 never stops. However, the results presented here show that both resistance loci are
732 still useful. Furthermore, the possibility of different mechanisms behind the
733 perception of the pathogen make these resistances very interesting for breeders.
734 With the genetic markers presented here, breeders can easily track the resistance
735 locus *Ren9* in further breeding lines.

736

737

738

739

740

741

742

743

744

745

746

747

748

749

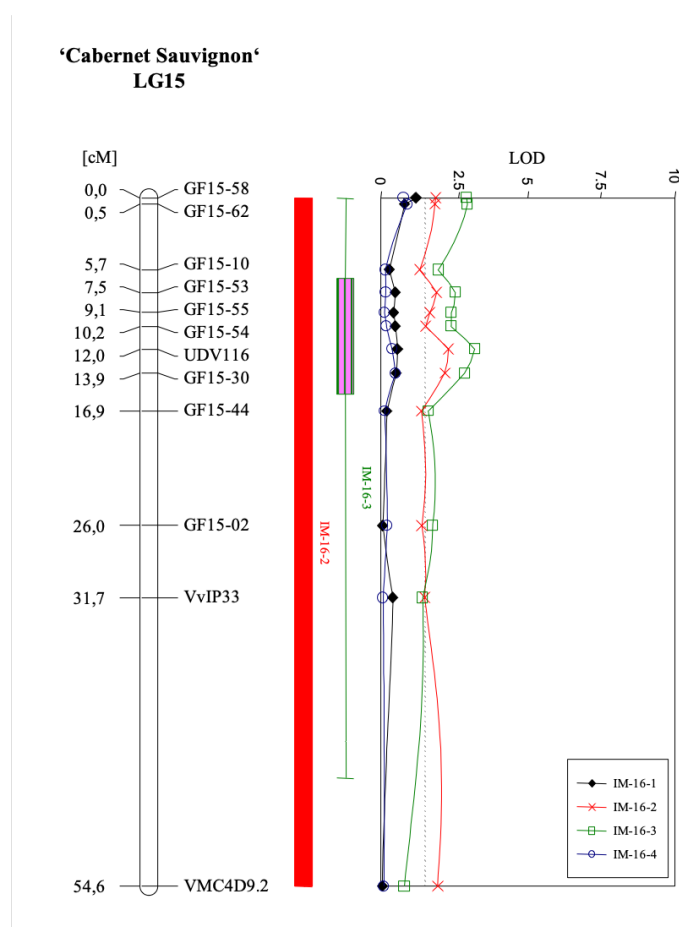
750

751

752

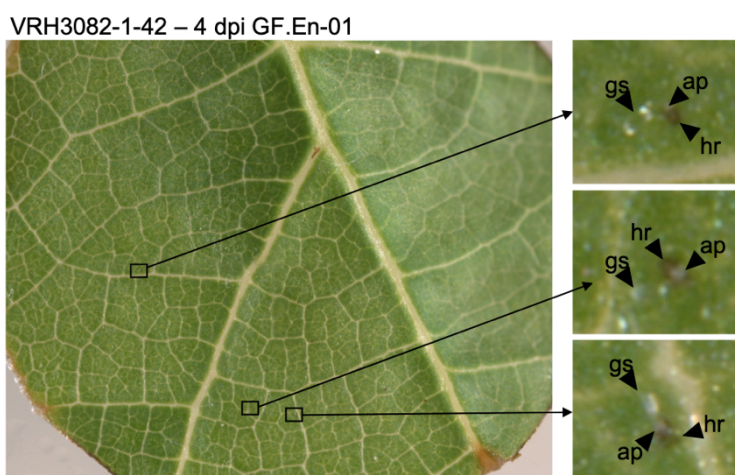
753

754 Supplementary Materials



755

756 Figure S 1: QTL-analysis results for the 'Cabernet Sauvignon' haplophase. Results for all four field-scoring are
757 plotted in one graph. The genetic map is given on the left. Significance threshold is 1.2 -1.3 as it was for the
758 'Regent' haplophase. $LOD_{max\pm 1}$ and 2 confidence intervals are indicated by boxes and their whiskers next to the
759 QTL-graph.



760

761 Figure S 2: Leaf disc of VRH3082-1-42 (*Run1*) inoculated with GF.En-01 four days past inoculation. Magnified
762 areas show germinated conidiospores (gs) with appressoria (ap) and a hypersensitive response (hr) associated
763 with it.

764

765 Table S1: Primer sequences used to amplify the newly designed Indel-maker. Together with the primer
766 sequences amplicon lengths and sequences of Regent (Cham='Chambourcin' haplophase, Dia='Diana'
767 haplophase', PN40024 12xv2 and 'Cabernet Sauvignon' v1.1 are given.

768 Table S2: Results of artificial inoculations of leaf discs with PM isolate GF.En-01. This table can be used with
769 the supplied R script to reproduce the graph.

770 Table S3: Data used for correlation plots. This data is for the first experiment (GFEn-01_1). Use the supplied R
771 script to reproduce the graph.

772 Table S4: Data used for correlation plots. This data is for the first experiment (GFEn-01_2). Use the added R
773 script to reproduce the graph.

774 Table S5: Data used for spore count plot to characterize GF.En-01 on 'Regent' and 'Chardonnay'.

775 Table S6: Data used to generate the fungal biomass increase plot to characterize the growth of GF.En-01 on
776 'Regent' and 'Chardonnay'.

777 Table S7: OIV455 field scoring data from 2016 used in Figure 2.

778

779 **Author Contributions:** D.Z. formal analysis, investigation, methodology, visualization and writing (original draft).
780 R.T. resources, writing (review & editing). E.Z. funding acquisition, planning, supervision, writing (review &
781 editing). All authors have read and approved the final manuscript.

782 **Funding:** This project was funded by Deutsche Forschungsgemeinschaft (DFG; Zy11/9-1 and 9-2)

783 **Acknowledgments:** Margit Schneider, Sissy Schatt and Claudia Welsch contributed expert technical
784 assistance. We wish to thank Margit Harst and Charlotte Mock for the provision of *in vitro* plants.

785 **Conflicts of Interest:** The authors declare no conflict of interest. The funders had no role in the design of the
786 study; in the collection, analyses, or interpretation of data; in the writing of the manuscript, or in the decision to
787 publish the results.

788

789

790

791

792

793

794

795

796

797

798

799 References

- 800 1. Töpfer, R.; Hausmann, L.; Harst, M.; Maul, E.; Zyprian, E.; Eibach, R. New Horizons for
801 Grapevine Breeding. In *Fruit, Vegetable and Cereal Science and Biotechnology*; 2011; pp. 79–96
802 ISBN 978-4-903313-75-7.
- 803 2. Dry, I.; Riaz, S.; Fuchs, M.; Sosnowski, M.; Thomas, M. Scion Breeding for Resistance to Biotic
804 Stresses. In *The Grape Genome*; Cantu, D., Walker, M.A., Eds.; Springer, 2019; pp. 319–347.
- 805 3. Gadoury, D.M.; Cadle-Davidson, L.; Wilcox, W.F.; Dry, I.B.; Seem, R.C.; Milgroom, M.G.
806 Grapevine powdery mildew (*Erysiphe necator*): A fascinating system for the study of the
807 biology, ecology and epidemiology of an obligate biotroph. *Mol. Plant Pathol.* **2012**, *13*, 1–16,
808 doi:10.1111/j.1364-3703.2011.00728.x.
- 809 4. Wilcox, W.F.; Gubler, W.D.; Uyemoto, J.K. PART I: Diseases Caused by Biotic Factors. In
810 *Compendium of Grape Diseases, Disorders, and Pests, Second Edition*; Wilcox, W.F., Gubler, W.D.,
811 Uyemoto, J.K., Eds.; The American Phytopathological Society, 2015; pp. 17–146.
- 812 5. Powell, K.S. A Holistic Approach to Future Management of Grapevine Phylloxera. In
813 *Arthropod Management in Vineyards: Pests, Approaches, and Future Directions*; Springer
814 Netherlands: Dordrecht, 2012; pp. 219–251 ISBN 9789400740327.
- 815 6. Johnson, G.F. The Early History of Copper Fungicides. *Agric. Hist.* **1935**, *9*, 67–79.
- 816 7. Chen, M.; Brun, F.; Raynal, M.; Makowski, D. Delaying the first grapevine fungicide
817 application reduces exposure on operators by half. *Sci. Rep.* **2020**, *10*, 1–12, doi:10.1038/s41598-
818 020-62954-4.
- 819 8. Commission, E. *The use of plant protection products in the European Union Data 1992-2003 2007*
820 *edition*; 2007; ISBN 92-79-03890-7.
- 821 9. García-Esparza, M.A.; Capri, E.; Pirzadeh, P.; Trevisan, M. Copper content of grape and wine
822 from Italian farms. *Food Addit. Contam.* **2006**, *23*, 274–280, doi:10.1080/02652030500429117.
- 823 10. Provenzano, M.R.; El Bilali, H.; Simeone, V.; Baser, N.; Mondelli, D.; Cesari, G. Copper
824 contents in grapes and wines from a Mediterranean organic vineyard. *Food Chem.* **2010**, *122*,
825 1338–1343, doi:10.1016/j.foodchem.2010.03.103.
- 826 11. Ballabio, C.; Panagos, P.; Lugato, E.; Huang, J.H.; Orgiazzi, A.; Jones, A.; Fernández-Ugalde,
827 O.; Borrelli, P.; Montanarella, L. Copper distribution in European topsoils: An assessment
828 based on LUCAS soil survey. *Sci. Total Environ.* **2018**, *636*, 282–298,
829 doi:10.1016/j.scitotenv.2018.04.268.
- 830 12. Pertot, I.; Caffi, T.; Rossi, V.; Mugnai, L.; Hoffmann, C.; Grando, M.S.; Gary, C.; Lafond, D.;
831 Duso, C.; Thiery, D.; et al. A critical review of plant protection tools for reducing pesticide use
832 on grapevine and new perspectives for the implementation of IPM in viticulture. *Crop Prot.*

- 833 **2017**, 97, 70–84, doi:10.1016/j.cropro.2016.11.025.
- 834 13. Qiu, W.; Feechan, A.; Dry, I. Current understanding of grapevine defense mechanisms against
835 the biotrophic fungus (*Erysiphe necator*), the causal agent of powdery mildew disease. *Hortic.*
836 *Res.* **2015**, 2, doi:10.1038/hortres.2015.20.
- 837 14. Zyprian, E.; Ochßner, I.; Schwander, F.; Šimon, S.; Hausmann, L.; Bonow-Rex, M.; Moreno-
838 Sanz, P.; Grando, M.S.; Wiedemann-Merdinoglu, S.; Merdinoglu, D.; et al. Quantitative trait
839 loci affecting pathogen resistance and ripening of grapevines. *Mol. Genet. Genomics* **2016**, 291,
840 1573–1594, doi:10.1007/s00438-016-1200-5.
- 841 15. Zendler, D.; Schneider, P.; Töpfer, R.; Zyprian, E. Fine mapping of Ren3 reveals two loci
842 mediating hypersensitive response against *Erysiphe necator* in grapevine. *Euphytica* **2017**, 213,
843 68, doi:10.1007/s10681-017-1857-9.
- 844 16. Cadle-Davidson, L.; Londo, J.; Martinez, D.; Sapkota, S.; Gutierrez, B. From Phenotyping to
845 Phenomics: Present and Future Approaches in Grape Trait Analysis to Inform Grape Gene
846 Function. In *The Grape Genome*; 2019; pp. 199–222.
- 847 17. Frenkel, O.; Portillo, I.; Brewer, M.T.; Péros, J.P.; Cadle-Davidson, L.; Milgroom, M.G.
848 Development of microsatellite markers from the transcriptome of *Erysiphe necator* for
849 analysing population structure in North America and Europe. *Plant Pathol.* **2012**, 61, 106–119,
850 doi:10.1111/j.1365-3059.2011.02502.x.
- 851 18. Agurto, M.; Schlechter, R.O.; Armijo, G.; Solano, E.; Serrano, C.; Contreras, R.A.; Zúñiga, G.E.;
852 Arce-Johnson, P. RUN1 and REN1 Pyramiding in Grapevine (*Vitis vinifera* cv. Crimson
853 Seedless) Displays an Improved Defense Response Leading to Enhanced Resistance to
854 Powdery Mildew (*Erysiphe necator*). *Front. Plant Sci.* **2017**, 8, 1–15, doi:10.3389/fpls.2017.00758.
- 855 19. Feechan, A.; Anderson, C.; Torregrosa, L.; Jermakow, A.; Mestre, P.; Wiedemann-Merdinoglu,
856 S.; Merdinoglu, D.; Walker, A.R.; Cadle-Davidson, L.; Reisch, B.; et al. Genetic dissection of a
857 TIR-NB-LRR locus from the wild North American grapevine species *Muscadinia rotundifolia*
858 identifies paralogous genes conferring resistance to major fungal and oomycete pathogens in
859 cultivated grapevine. *Plant J.* **2013**, 76, 661–674, doi:10.1111/tpj.12327.
- 860 20. Feechan, A.; Kocsis, M.; Riaz, S.; Zhang, W.; Gadoury, D.M.; Walker, M.A.; Dry, I.B.; Reisch,
861 B.; Cadle-Davidson, L. Strategies for RUN1 Deployment Using RUN2 and REN2 to Manage
862 Grapevine Powdery Mildew Informed by Studies of Race Specificity. *Phytopathology* **2015**, 105,
863 1104–1113, doi:10.1094/PHYTO-09-14-0244-R.
- 864 21. Veikondis, R.; Burger, P.; Vermeulen, A.K.; Van Heerden, C.J.; Prins, R. Confirmation of the
865 effectiveness and genetic positions of disease resistance loci in ‘Kishmish Vatkana’ (*Ren1*) and
866 ‘Villard Blanc’ (*Ren3* and *Rpv3*). *South African J. Enol. Vitic.* **2018**, 39, 185–195, doi:10.21548/39-
867 2-2685.
- 868

- 869 22. Teh, S.L.; Fresnedo-Ramírez, J.; Clark, M.D.; Gadoury, D.M.; Sun, Q.; Cadle-Davidson, L.;
870 Luby, J.J. Genetic dissection of powdery mildew resistance in interspecific half-sib grapevine
871 families using SNP-based maps. *Mol. Breed.* **2017**, *37*, 1, doi:10.1007/s11032-016-0586-4.
- 872 23. van Heerden, C.J.; Burger, P.; Vermeulen, A.; Prins, R. Detection of downy and powdery
873 mildew resistance QTL in a 'Regent' × 'RedGlobe' population. *Euphytica* **2014**, *200*, 281–295,
874 doi:10.1007/s10681-014-1167-4.
- 875 24. Csikós, A.; Németh, M.Z.; Frenkel, O.; Kiss, L.; Váczy, K.Z. A fresh look at grape powdery
876 mildew (*Erysiphe necator*) a and b genotypes revealed frequent mixed infections and only b
877 genotypes in flag shoot samples. *Plants* **2020**, *9*, 1–12, doi:10.3390/plants9091156.
- 878 25. Zini, E.; Dolzani, C.; Stefanini, M.; Gratl, V.; Bettinelli, P.; Nicolini, D.; Betta, G.; Dorigatti, C.;
879 Velasco, R.; Letschka, T.; et al. R-Loci Arrangement Versus Downy and Powdery Mildew
880 Resistance Level: A Vitis Hybrid Survey. *Int. J. Mol. Sci.* **2019**, *20*, 3526,
881 doi:10.3390/ijms20143526.
- 882 26. Gadoury, D.M.; Seem, R.C.; Ficke, A.; Wilcox, W.F. Ontogenic resistance to powdery mildew
883 in grape berries. *Phytopathology* **2003**, *93*, 547–555, doi:10.1094/PHYTO.2003.93.5.547.
- 884 27. Ficke, A.; Gadoury, D.M.; Seem, R.C.; Godfrey, D.; Dry, I.B. Host barriers and responses to
885 *Uncinula necator* in developing grape berries. *Phytopathology* **2004**, *94*, 438–445,
886 doi:10.1094/PHYTO.2004.94.5.438.
- 887 28. Lolle, S.; Stevens, D.; Coaker, G. Plant NLR-triggered immunity: from receptor activation to
888 downstream signaling. *Curr. Opin. Immunol.* **2020**, *62*, 99–105.
- 889 29. Baggs, E.; Dagdas, G.; Krasileva, K. V. NLR diversity, helpers and integrated domains: making
890 sense of the NLR IDentity. *Curr. Opin. Plant Biol.* **2017**, *38*, 59–67, doi:10.1016/j.pbi.2017.04.012.
- 891 30. Heese, A.; Hann, D.R.; Gimenez-Ibanez, S.; Jones, A.M.E.; He, K.; Li, J.; Schroeder, J.I.; Peck,
892 S.C.; Rathjen, J.P. The receptor-like kinase SERK3/BAK1 is a central regulator of innate
893 immunity in plants. *Proc. Natl. Acad. Sci. U. S. A.* **2007**, *104*, 12217–12222,
894 doi:10.1073/pnas.0705306104.
- 895 31. Zhu, K.; Wang, X.; Liu, J.; Tang, J.; Cheng, Q.; Chen, J.G.; Cheng, Z.M. The grapevine kinome:
896 Annotation, classification and expression patterns in developmental processes and stress
897 responses. *Hortic. Res.* **2018**, *5*, doi:10.1038/s41438-018-0027-0.
- 898 32. Jaillon, O.; Aury, J.M.; Noel, B.; Policriti, A.; Clepet, C.; Casagrande, A.; Choisne, N.; Aubourg,
899 S.; Vitulo, N.; Jubin, C.; et al. The grapevine genome sequence suggests ancestral
900 hexaploidization in major angiosperm phyla. *Nature* **2007**, *449*, 463–467,
901 doi:10.1038/nature06148.

902

903

- 904 33. Canaguier, A.; Grimplet, J.; Di Gaspero, G.; Scalabrin, S.; Duchêne, E.; Choisne, N.; Mohellibi,
905 N.; Guichard, C.; Rombauts, S.; Le Clainche, I.; et al. A new version of the grapevine reference
906 genome assembly (12X.v2) and of its annotation (VCost.v3). *Genomics Data* **2017**, *14*, 56–62,
907 doi:10.1016/j.gdata.2017.09.002.
- 908 34. Van Ooijen, J.W. JoinMap® 4, Software for the calculation of genetic linkage maps in
909 experimental populations 2006.
- 910 35. Jones, L.; Riaz, S.; Morales-Cruz, A.; Amrine, K.C.; McGuire, B.; Gubler, W.D.; Walker, M.A.;
911 Cantu, D. Adaptive genomic structural variation in the grape powdery mildew pathogen,
912 *Erysiphe necator*. *BMC Genomics* **2014**, *15*, 1081, doi:10.1186/1471-2164-15-1081.
- 913 36. Daudi, A. Detection of Hydrogen Peroxide by DAB Staining in *Arabidopsis* Leaves. *Bio protoc*
914 **2016**, *2*, 4–7.
- 915 37. Cadle-Davidson, L.; Gadoury, D.; Fresnedo-Ramirez, J.; Yang, S.; Barba, P.; Sun, Q.;
916 Demmings, E.M.; Seem, R.C.; Schaub, M.; Nowogrodzki, A.; et al. Lessons from a phenotyping
917 center revealed by the genome-guided mapping of powdery mildew resistance loci.
918 *Phytopathology* **2016**, *106*, 1159–1169, doi:10.1094/PHYTO-02-16-0080-FI.
- 919 38. R Core Team R: A Language and Environment for Statistical Computing 2019.
- 920 39. Kassambara, A. ggpubr: “ggplot2” Based Publication Ready Plots 2020.
- 921 40. Wei, T.; Simko, V. R package “corrplot”: Visualization of a Correlation Matrix 2017.
- 922 41. Van Ooijen, J.W. MapQTL ® 6, Software for the mapping of quantitative trait loci in
923 experimental populations of diploid species 2009.
- 924